

How to Cite:

Shehab, N. M., Abdelhady, A. A., Noaman, K. M., & Tawfeek, H. E. M. (2022). 3D finite element analysis assessment of maxillary premolar restored with various restorative materials. *International Journal of Health Sciences*, 6(S9), 908–921. <https://doi.org/10.53730/ijhs.v6nS9.12349>

3D finite element analysis assessment of maxillary premolar restored with various restorative materials

Nasser Mohey Shehab

Faculty of Dental Medicine, Al-Azhar University, Cairo, Egypt.
Corresponding author email: drn.shehab.86@gmail.com.

Abdullah Ahmed Abdelhady

Faculty of Dental Medicine, Al-Azhar University, Cairo, Egypt.

Khaled Mohammad Noaman

Faculty of Dental Medicine, Al-Azhar University, Cairo, Egypt.

Hossam El Mandouh Tawfeek

Conservative Dentistry Department, Faculty of Dentistry, Suez Canal University, Egypt.

Abstract---Objectives: The study used three-dimensional finite element analysis to evaluate the effects of total deformation and Von Mises stresses (VMS) of different shaped non-carious cervical lesions (NCCLs) and occluso-gingival dimensions (OGD) of maxillary premolars when restored with different restorative materials. Methods: Maxillary premolar was scanned utilizing 3D-laser scanning to produce a 3D digital geometrical model. Six cavities were created with three different shapes (notch, saucer, and mixed), and two OGD (1.5mm and 3mm). Two 100N oblique forces were applied at 11° and 45° from the vertical axis. The total deformation data obtained were expressed in mm, and the VMS values were recorded. Results: Various tested dimensions and shapes of NCCLs produce equivalent values of maximum total deformation on restorations. Increasing oblique angle from 11° to 45° increased the total deformation about three times. Increasing oblique angle increase VMS by about 30%. One Bulk Fill restorative came in second with the lowest VMS. Ketacã N100 restoration had the longest lifetime. Conclusion: Various OGD shapes of NCCLs did not affect the restoration deformation or the values of VMS, whereas the loading angle and the type of restorative materials influenced the stress distribution in the cavity models of the maxillary premolars.

Keywords--Finite element analysis, Maxillary premolar, Non-carious cervical lesions, Restorative materials, Stress distribution.

Introduction

Non-carious lesions are pathological defects in the hard tooth structure that are frequently seen in the buccal surface of teeth in the cervical region.^{1,2} These pathologic lesions are commonly seen in the clinical practice on the buccal surfaces of all dentitions from the canines to the molar teeth, but they are prevalent mostly in the premolar teeth, especially the first maxillary premolars.¹⁻⁴ Non-carious cervical lesions are of multifactorial etiology^{4,5} which may be arises due to the action of abnormal stresses and known as (abfraction), or action of wear (friction) as well as they could be resulted due to chemical, electrochemical, and biochemical degradation (biocorrosion), in addition, these defects could result from a combination of the previously mentioned conditions.^{1,2,4,6}

The multifactorial etiology of NCCLs results in defects of various morphologies in the cervical enamel (it is thin and more susceptible to generate defects) which can be categorized as notch-shape (NS), saucer-shape (SS), and mixed-shape (MS).^{1,7} The notch-shape defect is characterized by the existence of internal sharp line angle geometry, while the saucer-shape defect has an internal geometry of rounded line angle, however, the mixed-shape defect has an internal geometry that characterizes smooth and semi-circular occlusal wall lines, and acute gingival line angles.^{1,5}

Furthermore, different types of occlusal loads cause varied stress distribution patterns in the tooth's cervical enamel. Occlusal contacts and up-normal forces along the long axis of the tooth could be related to increased stresses (fatigue) in the cervical region of the rigid enamel structure and hence the development of cervical defects. Moreover, the continued exposure to these stresses in combination with the presence of the predisposing factors the further progression of the defect will occur.^{1,2} Furthermore, it was found that the severity of the NCCL increase with the age,⁸ also the dimension and number of these defects increase with age.^{1,8} Generally, the removal of the etiological factors of the NCCLs and/or replacement of the lost hard tooth structure can promote an enhancement in aesthetics and decrease the possible hypersensitivity which resulted because of these lesions.⁴ However, the restoration of NCCLs with different restorative materials is not considered an actual treatment for these types of hard tooth structure lesions.⁹

Among the available restorations for these lesions, it was found that the use of resin composites, glass-ionomer-based materials, and polyacid modified glass-ionomers (compomers) are useful restorations for these lesions.^{10,11} Methods used to simulate the tooth structures and their associated characteristics are usually useful to analyze the tooth behavior under various occlusal load conditions in case of structural loss, and the effects of the used restorative material(s), considering their properties.² The use of the FEA method to analyze the observed stresses under various stresses conditions could be useful in the evaluation of the different associated factors within the same model.¹² This study used 3-D finite

element analysis to assess and compare the effect of the morphology and size of NCCLs on stress distribution in maxillary premolars restored with different restorative materials.

Materials and Methods

Geometric Model production:

Six different "3-D finite element models" were produced in total, beginning with the 3D scanning of a test tooth (maxillary premolar). (2) A laser scanner was used to acquire the tooth geometry (Geomagic Capture, 3D Systems, Cary, NC, USA). Such a scanner generated a data file with a cloud of coordinates points (**Figure. 1**). To trim a newly produced surface by the acquired points, intermediary software (Rhino 3.0 - McNeel Inc., Seattle, WA, USA) was necessary. The solid (closed) tooth shape was then exported as a STEP file format to the finite element application.

Six cavities with 3 different shapes (notch, saucer, and mixed) and 2 OGDs (1.5 and 3-mm) were created to simulate the removed geometry from crown/tooth to create the final shape for cavities and placement of restorative materials. Each NCCL shape was simulated in two conditions/sizes minor (1-mm depth from tooth surface) and severe (2-mm depth from tooth surface), thus cavity height (OGD) increased from 1.5 to 3-mm (**Figure. 2**).



Figure. 1: (a) Laser scanner; (b) scanned tooth as a cloud of points; (c) scanned tooth after creating its surface

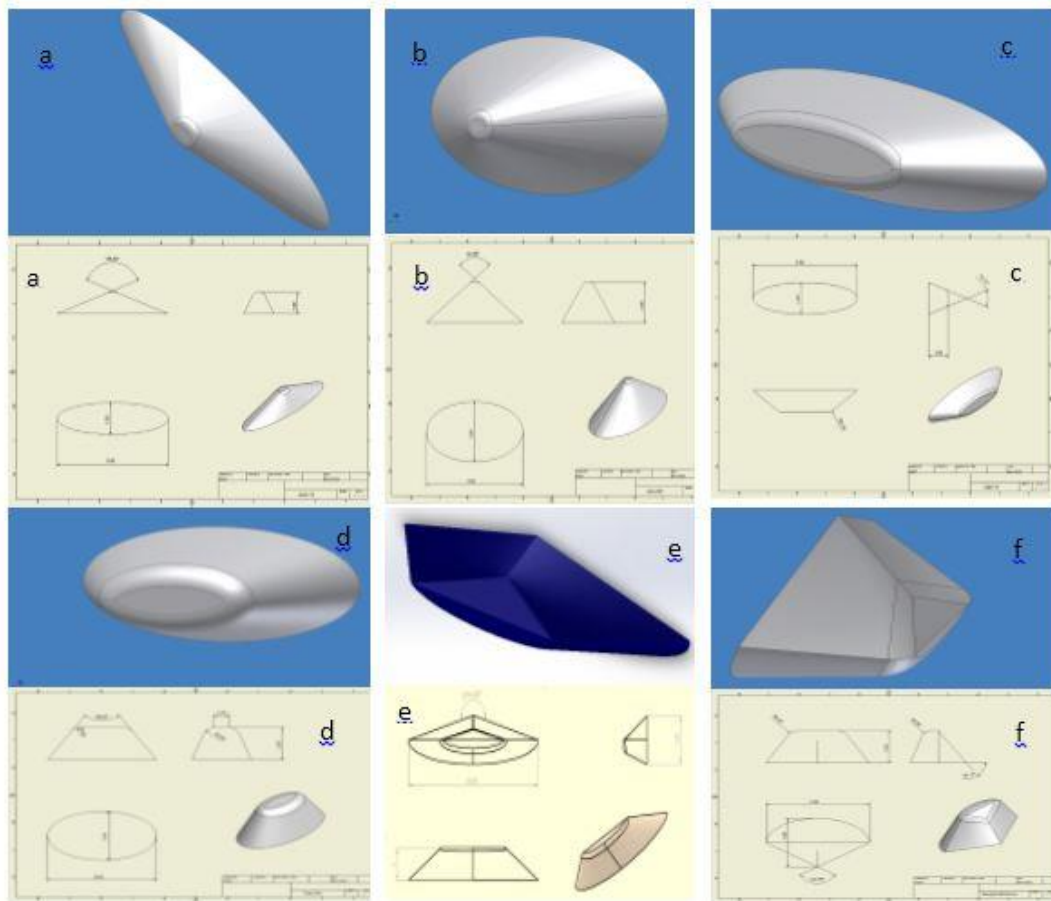


Figure 2: Dimensions and geometry of the cutting volume to form the tooth palatal side; (a) cone 15, (b) cone 30, (c) tube 15, (d) tube 30, (e) mixed cavity 15, and (f) mixed cavity 30.

Two coaxial cylinders were used to simulate the bone shape. The interior cylinder, which measures 14 mm in diameter and 22 mm in height, represents the trabecular bone. (3) The outer cylinder, which has a shell that is 1 mm thick, depicts the cortical bone (16-mm exterior diameter, 24-mm height). On the engineering CAD/CAM programme "Autodesk Inventor," version 8, both the cylinder and cavity models were produced in three dimensions (Autodesk Inc., San Rafael, CA, USA). To build the final necessary models, a series of Boolean operations were performed on the finite element package. (Figure. 3). The cementum layer of 800-1000 microns around the root was ignored in these designs.

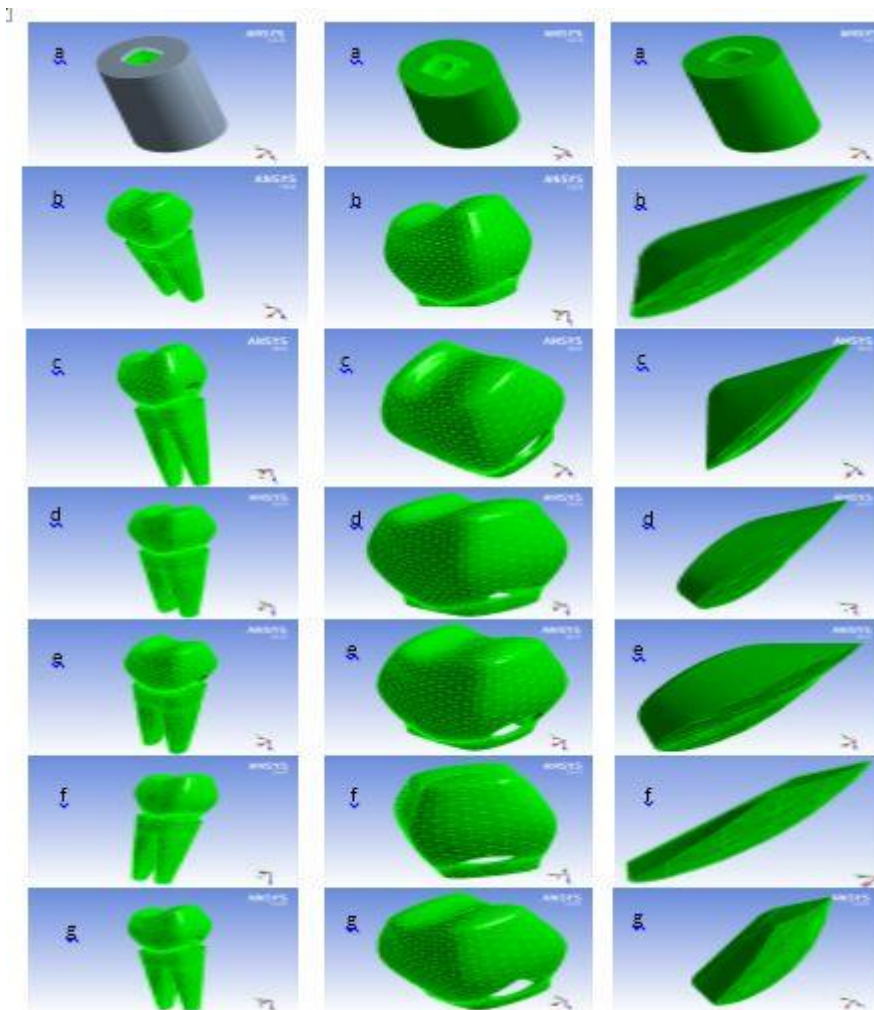


Figure 3: Final models' parts from ANSYS screens (a) cortical and spongy bone, which is the same all tooth models, (b) Model #1: notch 1.5mm, (c) Model #2: notch 3mm, (d) Model #3: saucer 1.5mm, (e) Model #4: saucer 3mm, (f) Model #5: Mixed 1.5mm, and (g) Model #6: Mixed 3mm

After applying a set of Boolean operations (add, subtract, overlap, etc) the models' parts were ready for material assignment and meshing. Thus model #1 can be defined as notch cavity 1.5mm, model #2 as notch cavity 3mm, model #3 as saucer cavity 1.5mm, model #4 as saucer cavity 3mm, model #5 as mixed cavity 1.5mm, and model #6 as mixed cavity 3mm. These cavities were made to be filled with one of the three evaluated restorative materials, Nano-filled Resin modified glass ionomer cement (Ketac Nano 100 light-curing glass ionomer restorative 3M ESPE, St Paul, MN, USA), Bulk fill resin composite (One Bulk Fill restorative 3M ESPE, St Paul, MN, USA), and Nano-hybrid resin composite (Filtek Z350 XT 3M ESPE, St Paul, MN, USA). All of the materials employed in this investigation were definitionally homogeneous, isotropic, and elastic along a linear direction.

Definition of the material properties:

Two essential parameters must be determined for linear static stress analysis: elastic (Young's) modulus and Poisson's Ratio, which are sufficient for defining the linear component of an isotropic material's stress-strain curve. The properties of the used materials were listed in Table 1.

Table 1: Material properties of models' component

Material	Modulus of elasticity in MPa	Poisson's ratio
Cortical	13,700	0.30
Spongy	1,370	0.30
Enamel	80,350	0.33
Dentin	19,890	0.31
Filtek Z350 XT	11,348	0.30
Bulk-fill posterior	9,348	0.30
Ketacä N100	4,000	0.35

Mesh creation (conception of nodes and elements):

Each model component had a material property assigned to it using the ANSYS Workbench version 16 finite element programme (ANSYS Inc., Canonsburg, PA, USA). The model was then meshed using a parabolic tetrahedral element, with an appropriate mesh density chosen to guarantee accurate results for the discrete model. Table 2,3 show the mesh density of all model elements.

Table 2 showed the number of nodes and elements in all meshed components from models #1, #2, and #3.

Model #no	Model #1		Model #2		Model #3	
Component	Nodes	Elements	Nodes	Elements	Nodes	Elements
Cortical	49,692	30,917	49,692	30,917	49,692	30,917
Spongy	177,528	125,875	177,528	125,875	177,528	125,875
Dentin (Root + Crown)	308,823	214,760	314,986	219,163	329,187	230,713
Crown						
Enamel	170,383	113,564	168,670	112,442	169,751	113,054
Restoration	7,740	4,903	16,210	10,625	752,450	518,145

Table 3: Number of nodes and elements in all meshed components from models #4, #5, #6

Model #no	Model #4		Model #5		Model #6	
Component	Nodes	Elements	Nodes	Elements	Nodes	Elements
Cortical	49,692	30,917	49,692	30,917	49,692	30,917
Spongy	177,528	125,875	177,528	125,875	177,528	125,875
Dentin (Root + Crown)	313,323	218,149	322,595	224,898	322,170	224,715
Crown						

Enamel	170,703	114,105	177,826	118,643	173,187	115,798
Restoration	20,780	14,158	15,962	10,850	18,131	12,268

Another important element is mesh density. Because the geometries are complicated, enhancing the mesh has the expected effect of improving the discrete model results (increasing the obtained stress levels accuracy in regions of high-stress gradients). Another benefit of increasing the number of elements is that it reduces artificially manufactured sharp angles caused by the process of substituting the geometric model by the mesh, hence reducing artificial peak stresses by better the representation of the true geometry. Mesh density was investigated and adjusted in terms of accuracy and calculation time. Meshed components as screenshots of the six models are presented in (figure. 4).

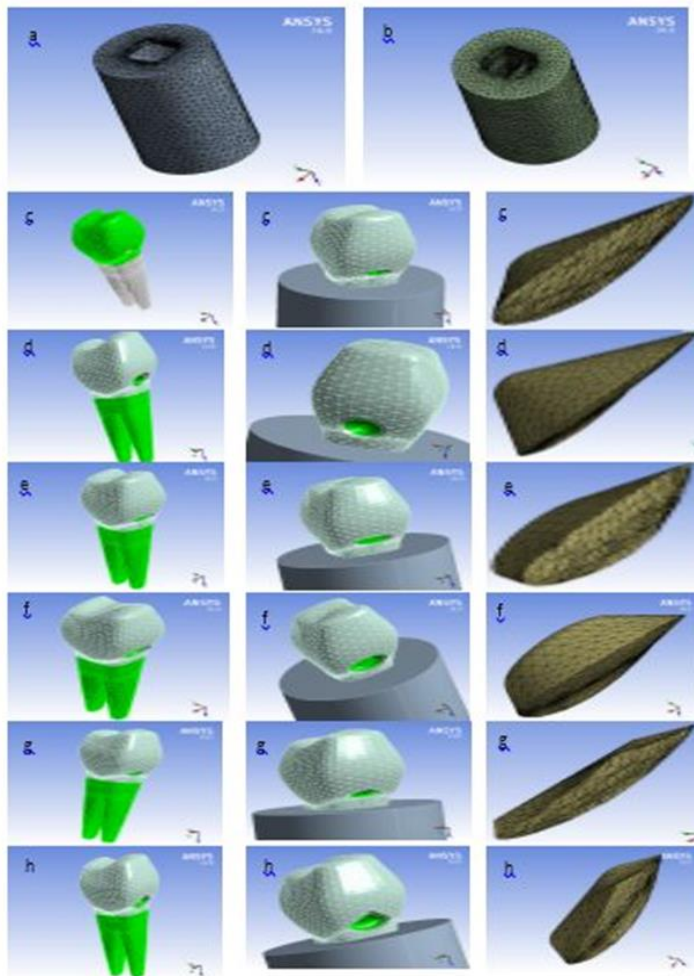


Figure 4: Meshed components; (a) cortical bone, (b) spongy bone, (c) Model #1: Cone 15, (d) Model #2: Cone 30, (e) Model #3: Tube 15, (f) Model #4: Tube 30, (g) Model #5: Mixed 15, (h) Model #6: Mixed 30.

Application of load and boundary conditions:

After the six models meshed, two different oblique forces each of 100N were applied as two load cases one at 11° and the other at 45° from the vertical axis. (23) Each load was equally divided into 5 points representing; palatal cusp tip, Mesial and distal marginal ridges, and palatal cusp slopes (**Figure. 5**).

As a result, the six models underwent a total of 36 runs (six on each model as two loading conditions on each of the three restoration materials). As a boundary condition, the hollow cylinder's base—which represented the cortical bone—was set to be fixed as a boundary condition. On a Workstation HP Z820 with Dual Intel Xeon E5-2660, 2.2 GHz CPUs, 64GB RAM, solid modelling and finite element analysis (linear static analysis) were carried out. Then, the resultant stresses and deformations were calculated under both loading conditions and presented as distributions. The distributions as; maximal resultant values in “red color”, while the minimum values were represented in “blue color”. These values were tabulated, compared, and discussed in the results.

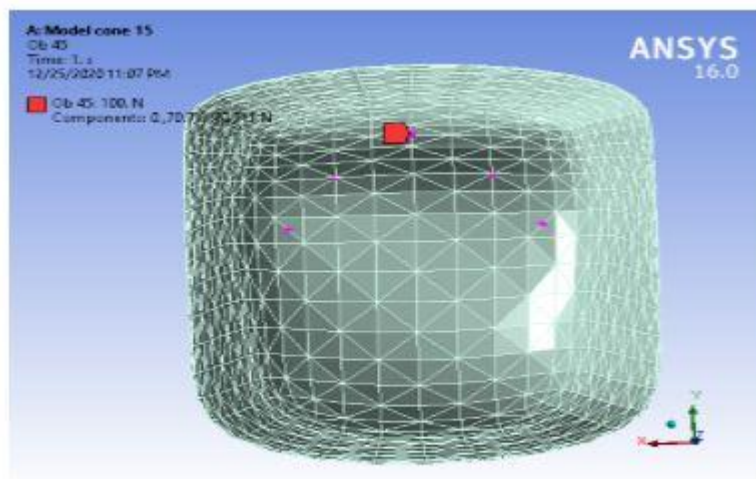


Figure 5: Loading points of tooth structure

Results

The results of all models showed that the maximum value of total deformation in palatal direction appeared at the occlusal margin (upper part of mesial corner) of the restorations, while the maximum value of Von Mises stresses in these models appeared at the cervical margin of the restorations. 36 runs were performed on the six models as following:

Model 1(notch shape with 1.5mm OGD cavity) restored by (**R1** Filtek z350 xt, under 100N oblique load of 11°, **R2** Filtek z350 xt, under 100N oblique load of 45°, **R3** Bulk fill posterior, under 100N oblique load of 11°, **R4** Bulk fill posterior, under 100N oblique load of 45°, **R5** Ketac Nano100, under 100N oblique load of

11°, R6 Ketac Nano100, under 100N oblique load of 45°). **Model 2**(notch shape with 3mm OGD cavity), **Model 3** (saucer shape with 1.5mm OGD cavity). **Model 4** (saucer shape with 3mm OGD cavity), **Model 5** (mixed shape with 1.5mm OGD cavity). **Model 6** (mixed shape with 3mm OGD cavity).

The results of notch shape defect with a cavity of 1.5-mm OGD at 11° oblique load of 100 N (model #1) showed that the maximum value of total deformation was recorded 0.0158 mm for all restorative materials. While the maximum value of VMS in this model recorded 4.3, 3.9, and 2.4 MPa for Filtek Z350 XT, Bulk-fill, and Ketacã N100 restorations respectively. However, the results of notch shape defect with a cavity of 1.5-mm OGD at 45° oblique load of 100 N (model #1) showed that the maximum value of total deformation was recorded 0.0462 mm for all restorative materials. While the maximum value of VMS in this model appeared at the cervical margin of the restoration and recorded 11.5, 10.3, and 6.4 MPa for Filtek Z350 XT, Bulk-fill, and Ketacã N100 restorations respectively.

Comparison between finite element Results:

In both loading scenarios, the finite element analysis of all evaluated models revealed stresses within physiological bounds. Supplemental figures compared maximum values total deformation and Von Mises stress on all parts of the studied models.

The results of notch shape defect with a cavity of 3-mm OGD at 11° oblique load of 100 N (model #2) showed that the maximum value of total deformation was recorded 0.0171 mm for all restorative materials. While the maximum value of VMS in this model was recorded 3.4, 3.3, and 1.7 MPa for Filtek Z350 XT, Bulk-fill, and Ketacã N100 restorations respectively. However, the results of notch shape defect with a cavity of 3-mm OGD at 45° oblique load of 100 N (model #2) showed that the maximum value of total deformation was recorded 0.0495 mm for all restorative materials. While the maximum value of VMS in this model appeared at the cervical margin of the restoration and recorded 10.2, 8.9, and 4.7 MPa for Filtek Z350 XT, Bulk-fill, and Ketacã N100 restorations respectively.

The results of saucer shape defect with a cavity of 1.5-mm OGD at 11° oblique load of 100 N (model #3) showed that the maximum value of total deformation was recorded 0.0296 mm for all restorative materials. While the maximum value of VMS in this model recorded 586.3 MPa for all restorations. However, the results of saucer shape defect with a cavity of 1.5-mm OGD at 45° oblique load of 100 N (model #3) showed that the maximum value of total deformation recorded 0.0751 mm for all restorative materials. While the maximum value of VMS in this model appeared at the cervical margin of the restoration and recorded 759.1 MPa for all restorations.

The results of saucer shape defect with a cavity of 3-mm OGD at 11° oblique load of 100 N (model #4) showed that the maximum value of total deformation was recorded 0.0296 mm for Filtek Z350 XT, and Bulk-fill restorative materials, and 0.0297 mm for Ketacã N100 restorative material. While the maximum value of VMS in this model recorded 580.2 MPa for Filtek Z350 XT, and Bulk-fill restorative materials, and 580.3 MPa for Ketacã N100 restorative material.

However, the results of saucer shape defect with a cavity of 3-mm OGD at 45° oblique load of 100 N (model #4) showed that the maximum value of total deformation recorded 0.0753 mm for Filtek Z350 XT, and Bulk-fill restorative materials, and 0.0755 mm for Ketacã N100 restorative material. While the maximum value of VMS in this model appeared at the cervical margin of the restoration and recorded 757.2 MPa for all restorations.

The results of mixed shape defect with a cavity of 1.5-mm OGD under a 11° oblique load of 100 N (model #5) showed that the maximum value of total deformation was recorded 0.0296 mm for all restorative materials. While the maximum value of VMS in this model recorded 581.9 MPa for all restorations. However, the results of mixed shape defect with a cavity of 1.5-mm OGD under 45° oblique load of 100 N (model #5) showed that the maximum value of total deformation recorded 0.0751 mm for Filtek Z350 XT, and Bulk-fill restorative materials, and 0.0752 mm for Ketacã N100 restorative material. While the maximum value of VMS in this model appeared at the cervical margin of the restoration and recorded 754.6 MPa for all restorations.

The results of mixed shape defect with a cavity of 3-mm OGD under a 11° oblique load of 100 N (model #6) showed that the maximum value of total deformation was recorded 0.0296 mm for Filtek Z350 XT, and Bulk-fill restorative materials, and 0.0297 mm for Ketacã N100 restorative material. While the maximum value of VMS in this model recorded 590.5 MPa for all restorations. However, the results of mixed shape defect with a cavity of 3-mm OGD under 45° oblique load of 100 N (model #6) showed that the maximum value of total deformation recorded 0.0754 mm for Filtek Z350 XT, and Bulk-fill restorative materials, and 0.0756 mm for Ketacã N100 restorative material. While the maximum value of VMS in this model appeared at the cervical margin of the restoration and recorded 882.4 MPa for Filtek Z350 XT, and Bulk fill restorative materials, and 882.5 MPa for Ketacã N100 restorative material.

Discussion

The results of the present study showed that the cavity shapes or sizes of NCCLs in the different tested models produce equivalent values of maximum total deformation on restorations under any case of the studied oblique loading. Increasing oblique angle from 11° to 45° increased the total deformation about three times. Considerable differences appeared between extreme values among maximum values of VMS on restorations. Increasing oblique angle increase VMS by about 30%. Ketacã N100 restoration showed the lowest VMS, followed by Bulk fill, then Filtek Z 350 XT received the highest values of VMS. Differences varied from about 10 to 45% which indicated the longest lifetime for Ketacã N100 restoration. To simulate the tooth structures in case of structural loss, and to simulate the compensation of this lost tooth structure with restorative materials, considering their properties, the use of the FEA method could be useful in the evaluation of the behavior of tooth and restoration under different occlusal stresses and their associated factors within the same model. ^{2,13} Values from FEA are categorized as VMS, shear stress, maximum principal stress which represents “tensile stress”, and minimum principal stress which represents “compressive stress”. ¹⁴ VMS was selected as a measure for analyzing the pattern of stress

distribution in the present study because it denotes the criterion of tensile stresses and seems to be reliable to analyzing the brittle materials, tooth, or restoration in the current study, which fail primarily due to the tensile type of stress.¹⁵

The oblique loads at 11° and 45° along long axis of the tooth models were selected in the present study to simulate the normal occlusal interference on the palatal and buccal slopes respectively of the maxillary premolars.¹⁶ While the vertical load was equally distributed on both buccal and palatal cusps of the maxillary premolar; therefore, this loading type simulates homogeneous distribution during contact,² thus this loading type was ignored in this study.

In the present study, the first maxillary premolar was selected to create the tooth model in case of the presence of NCCL defects this because these types of lesions are commonly seen with higher prevalence in the clinical practice on the buccal surfaces of the first maxillary premolars.¹⁻⁴ The selection of defect morphologies of NCCLs in the present study was based on clinical observation and previous studies that categorized the various morphologies of NCCLs as notch-shape (NS), saucer-shape (SS), and mixed-shape (MS).^{7,17} Furthermore, to replicate the oral environment and dimension of NCCLs, this study was done to evaluate NCCLs of 1.5 and 3-mm OGDs to determine the impact of NCCL on the restoration. NCCLs with depths of 1.5 mm should be regarded borderline when deciding whether or not to install a conservative restoration.¹ In the present study both OGD and shape of NCCLs has no significant effect on total deformation and VMS of restorative materials used in this study, This result is consistent with a prior work by Browning, who found that despite different cavity shapes and the resulting interfacial tension, the mechanical properties of the composite employed are mostly insignificant.²⁵ while the result was disagrees with the previous study by Zeola, L. F. who reported that the depth of NCCLs increases the magnitude and extent of stress concentration.¹⁸

The resin-based adhesive restorations were selected in the present study to restore the NCCLs because they are considered an effective replacement for the lost tooth structures in that they can enhance the aesthetics and help in the decrease of tooth hypersensitivity.² Moreover, resin-based restorative materials have elastic moduli resembling tooth dentine, which is sufficient to offset the generated stress by occlusal forces.¹²

Regarding the analyzed aspects in this study including the sizes and shapes NCCLs, their restorations, and direction of load were considered variables that affect the patterns of stress distribution in the maxillary premolar's models. According to the results of the present study, the different shapes of the NCCLs in the maxillary premolar models had an equivalent effect on the maximum total deformation of the three tested restorations under any case of the studied oblique loading. These results follow Soares et al in 2015, who reported that the morphology of NCCLs has a minimum effect on the pattern of stress distributions.²

Moreover, the results of the present study demonstrated that the direction of load and the type of restoration used in the NCCLs cavity are major factors in

modifying the patterns of stress distribution. This could be related to the oblique loading direction which used in this study and able to produce higher stress concentrations in the cervical region on the buccal and palatal surfaces of the tooth models. ^(2,10) Furthermore, the present study's findings showed that the maximum value of VMS in these tested models occurred at the cervical margin of the restorations, which could be attributed to the concentration of stresses at the cervical areas of enamel and dentine.

Additionally, the results showed that the increase in oblique loading angle from 11° to 45° increased the total deformation of restoration about three times, and the maximum stress was recorded at the cervical region of all tested models. This finding could be attributed to the different load directions of occlusal contacts which could promote considerable changes in the magnitude of tensile stresses, especially in the cervical region of the cavity, which in follows initiates deformation or premature failure of the restoration.² The results of this investigation are consistent with those of a study by Rees JS, who found that oblique loads applied to the buccal or lingual cusp slopes' inner aspects produced the highest maximum primary stress values, ranging from 247 to 285•5 MPa. This was caused by the way the cusps of these teeth were functioning. The occlusal stresses applied close to the cusp tips were as far away from the fulcrum point of the "beam"—located at the intersection of the tooth's cervical region and the crest of the alveolar bone. The highest lateral deflection of the tooth was caused by these stresses.¹⁶

Also, the results of this study demonstrated that Ketacä N100 restoration showed the lowest VMS, followed by Bulk fill, then Filtek Z350 XT received the highest values of VMS, and differences in VMS varied from about 10 - 45% which indicated the longest lifetime for Ketacä N100 restoration. This finding could be attributed to the lower elastic modulus of Ketacä N100 restorative material when compared to the Bulk-fill and Filtek Z350 XT. The lower elastic modulus of the restorative material can create areas of elastic bonding at the tooth-resin interface which have been proposed to act as an inherent buffer that offset the occlusal stresses on the restoration. This result is consistent with findings from a study by Sreirekha et al., who came to the conclusion that while materials with higher mechanical and elastic properties can support higher loads and resist wear, materials with lower elastic moduli are effective in abfraction lesions at low tensile stresses.¹⁹ Additionally, the results of our investigation agree with those of a prior study by Priyadarshini, B. I., et al., which found that Giomer restorations had greater colour matching and surface polish while Ketac Nano and RMGIC restorations were better preserved in NCCLs.²⁰ However, the Bulk-fill resin composite also receives a lower VMS when compared to Filtek Z350 XT in this present study because the Bulk-fill resin composite has relatively lowered viscosity and higher flexibility that promotes the stress-relief function and acts as a shock absorber than the traditional resin composites.^{21,22}

Conclusions

The results demonstrated that:

1. The main factors affecting the behavior of restoration were loading direction and type of restoration.

2. Various NCCLs shapes and sizes demonstrated equivalent effects on the amount of total deformation of the restorations and the values of VMS.
3. Increasing the oblique load from 11° to 45° showed increase in total deformation and VMS in the restorations.
4. The Ketac[®] N100 restoration showed lower VMS when compared to the Bulk-fill Filtek and Z350 XT resin composites regardless of the morphology of NCCLs.

References

1. Burrow MF, Tyas MJ. A clinical trial comparing two all-in-one adhesive systems used to restore non-cariious cervical lesions: Results at one year. *Aust Dent J* 2008; 53: 235–238.
2. Dejak B, Młotkowski A. Finite element analysis of strength and adhesion of cast posts compared to glass fiber-reinforced composite resin posts in anterior teeth. *J Prosthet Dent* 2011; 105 2: 115–126.
3. Du JK, Wu JH, Chen PH, Ho PS, Chen KK. Influence of cavity depth and restoration of non-cariious cervical root lesions on strain distribution from various loading sites. *BMC Oral Health* 2020; 20: 1–10.
4. Fron H, Vergnes J-N, Moussally C *et al.* Effectiveness of a new one-step self-etch adhesive in the restoration of non-cariious cervical lesions: 2-Year results of a randomized controlled practice-based study. *Dent Mater* 2011; 27: 304–312.
5. Grippo JO, Simring M, Coleman TA. Abfraction, abrasion, biocorrosion, and the enigma of noncariious cervical lesions: A 20-year perspective. *J Esthet Restor Dent* 2012; 24: 10–23.
6. Hur B, Kim HC, Park JK, Versluis A. Characteristics of non-cariious cervical lesions - an ex vivo study using micro computed tomography. *J Oral Rehabil* 2011; 38: 469–474.
7. Kamaluddin. (2021). Government and Private Collaboration in Coping with Covid-19 in Sorong City. *International Research Journal of Management, IT and Social Sciences*, 8(5), 333-341. <https://doi.org/10.21744/irjmis.v8n5.1907>
8. Martini, I. A. O., Lasmi, N. W., Jaya, N., & Sutrisni, N. K. E. (2017). Improving cooperative performance through human resource development efforts. *International Journal of Social Sciences and Humanities*, 1(3), 49–58. <https://doi.org/10.29332/ijssh.v1n3.55>
9. Mauricio F, Medina J, Vilchez L, Sotomayor O, Muricio-Vilchez C, Mayta-Tovalino F. Effects of Different Light-curing Modes on the Compressive Strengths of Nanohybrid Resin-based Composites: A Comparative In Vitro Study. *J Int Soc Prev Community Dent* 2021; 11: 184–189.
10. Priyadarshini B, Jayaprakash T, Nagesh B, Sunil C, Sujana V, Deepa V. One-year comparative evaluation of Ketac Nano with resin-modified glass ionomer cement and Giomer in noncariious cervical lesions: A randomized clinical trial. *J Conserv Dent* 2017; 20: 204–209.
11. Rees JS. The effect of variation in occlusal loading on the development of abfraction lesions: a finite element study. *J Oral Rehabil* 2002; 29: 188–193.
12. Rehman AUR, Naeem S, Rehman S, Ali A. Comparison of Composite Resin and Resin Modified Glass Ionomer Restorations on Dentinal Hypersensitivity in Non-Cariious Cervical Lesions. *Pakistan Oral Dent J* 2019; 39: 281–285.

13. Rizzante FAP, Duque JA, Duarte MAH, Mondelli RFL, Mendonça G, Ishikiriama SK. Polymerization shrinkage, microhardness and depth of cure of bulk fill resin composites. *Dent Mater J* 2019; 38: 403–410.
14. Rodrigues FAM. Ceramic onlay: influence of the deep margin elevation technique on stress distribution: a finite element analysis. 2016.
15. Senawongse P, Pongprueksa P, Tagami J. The effect of the elastic modulus of low-viscosity resins on the microleakage of Class V resin composite restorations under occlusal loading. *Dent Mater J* 2010; 29 3: 324–329.
16. Shetty S, Shetty R, Mattigatti S, Managoli N, Rairam S, Patil A. No Carious Cervical Lesions: Abfraction. *J Int oral Heal JIOH* 2013; 5: 143–146.
17. Silva LLC da, Pereira EKG, Silva DF da, Farias RR, Hora SL, Lins FC de R. Restorative treatment for non-carious cervical lesions – part 2. *Res Soc Dev* 2020; 9: e55991110236.
18. Soares P V., MacHado AC, Zeola LF *et al.* Loading and composite restoration assessment of various non-carious cervical lesions morphologies - 3D finite element analysis. *Aust Dent J* 2015; 60: 309–316.
19. Soares PV, Milito GA, Pereira FA *et al.* The effects of non carious cervical lesions - Morphology, load type and restoration - On the biomechanical behavior of maxillary premolars: A finite element analysis. *Biosci J* 2013; 29: 526–535.
20. Srirekha A, Bashetty K. A comparative analysis of restorative materials used in abfraction lesions in tooth with and without occlusal restoration: Three-dimensional finite element analysis. *J Conserv Dent* 2013; 16: 157–161.
21. Srirekha A, Bashetty K. Infinite to finite: An overview of finite element analysis. *Indian J Dent Res* 2010; 21: 425–432.
22. Suryasa, I. W., Rodríguez-Gámez, M., & Koldoris, T. (2022). Post-pandemic health and its sustainability: Educational situation. *International Journal of Health Sciences*, 6(1), i-v. <https://doi.org/10.53730/ijhs.v6n1.5949>
23. Wood ICJ, Jawad Z, Paisley CS, Brunton PA. Non-carious cervical tooth surface loss: a literature review. *J Dent* 2008; 36 10: 759–766.
24. Yarova SP, Zabolotna II, Genzytska O, Yarov Y, Makhnova A. The Correlation Of The Chemical Composition Of Enamel And Oral Fluid In Patients With A Wedge-Shaped Defect And Intact Teeth. *Georgian Med News* 2020; 309: 37–42.
25. Zeola LF, Pereira FA, Machado AC *et al.* Effects of non-carious cervical lesion size, occlusal loading and restoration on biomechanical behaviour of premolar teeth. *Aust Dent J* 2016; 61: 408–417.